Inorganica Chimica Acta 475 (2018) 35–46

Contents lists available at ScienceDirect

Inorganica Chimica Acta

journal homepage: www.elsevier.com/locate/ica

Urea-based flexible dicarboxylate linkers for three-dimensional metal-organic frameworks

Sebastian Glomb, Gamall Makhloufi, Irina Gruber, Christoph Janiak *

Institut für Anorganische Chemie und Strukturchemie, Heinrich-Heine-Universität Düsseldorf, 40204 Düsseldorf, Germany

ARTICLE INFO

Article history:
Received 30 June 2017
Received in revised form 7 September 2017
Accepted 11 September 2017
Available online 19 September 2017

Dedicated to Prof. Ionel Haiduc on the occasion of his 80th birthday.

Keywords:
MOFs, Metal-organic frameworks
Urea function
4,4′-(carbonylbis(azanediyl))dibenzoic acid
Interpenetration, fourfold
Diamondoid **dia** topology
Hydrogen bonding

ABSTRACT

The metal-organic frameworks (MOFs) 3D-$[Mn_2(L1)_2(DMF)]\cdot 2DMF$ (**1**), 3D-$[Cd_2(L2)_2(DMF)_3]$ (**3**), $[Zn_2(L2)_2(DMF)_3]$ (**4**) and 3D-$[Mn_2(L2)_2(DMF)_3]$ (**5**) are the first examples of three-dimensional metal-organic networks constructed from a single ditopic dicarboxylate linker (i.e., without bridging co-ligands) with an urea group in the linker axis ($L1^{2-}$ = 4,4′-(carbonylbis(azanediyl))dibenzoate; $L2^{2-}$ = 4,4′-(carbonylbis(azanediyl))bis(3-methylbenzoate), DMF = dimethylformamide). From $Cd^{2+}$and $L1^{2-}$ a 1D coordination polymer 1D-$[Cd(L1)(DMF)_3]$ (**2**) is formed. The urea group is engaged in hydrogen bonding with the C(4)[R_2^1(6)] motif to an oxygen atom of a DMF solvent (in **1**) or a metal-coordinated carboxylate group (in **3**–**5**). Network **1** has infinite channels with parallelepiped cross sections and 30% solvent-filled volume. The 3 D frameworks **3**–**5** are of diamond (6,6), **dia** topology with a single framework having large voids with 17.6 Å and 19.7 Å nodal separation. Thus, four symmetry-related nets interpenetrate, organized via H-bonds in the C(4)[R_2^1(6)] motif, still leaving about 50% solvent-filled void volume in the fourfold interpenetrated structure.

1. Introduction

Metal-organic frameworks (MOFs) attract continuous interest for their open network topologies associated with potential applications, mainly based on porosity and reversible guest exchange [1–3] with recently also water adsorption for heat transformation [4]. The interest in urea-based porous organic frameworks increased in the last years due to possible applications for hydrogen-bond-donating catalysis [5–7], anion recognition [8] and their high selectivity for CO_2 adsorption [9,10].

In the literature, there are only few examples known of MOFs with urea-functionalized carboxylate ligands [8,11,12] although the urea group with their H-bond donor and/or acceptor functions would be predestined for the separation of toxic gases such as SO_2, NH_3 or H_2S.

Possible and reported positions for the urea function in the linker can be in the main chain of the linker [8,12,13] or in the side chain of the ligand (Fig. 1) [5]. In the latter case, the urea function can also be introduced by postsynthetic modification [6,7].

Urea-based linkers with the urea group in the main chain are not rigid because of the rotational flexibility of the urea group that can assume different conformations. The synthesis of flexible MOFs is more dependent on reaction parameters such as solvent, temperature, concentration, pH etc. [14–16].

For all published syntheses of three-dimensional MOFs from linear urea-based dicarboxylate linkers, a further co-ligand had been required in order to obtain crystalline products for structure elucidation [8,11,12]. Roberts et al. [11] were the first to form a three-dimensional, porous urea-functionalized MOF (NU-601) by using the 5,5′-(carbonylbis(azanediyl))diisophthalate linker and 4,4′-bipyridine as co-ligand (Fig. 2). Tehrani et al. employed the ditopic 4,4′-(carbonylbis(azanediyl))dibenzoate ($L1^{2-}$) ligand and obtained with 4,4′-bipyridine (bipy), 1,2-bis(4-pyridyl)ethane (bpe) or 1,3-di(pyridin-4-yl)urea the mixed-ligand MOFs TMU-18, -19 [12] and -31 [8], respectively for the use as Lewis acid catalysts or for sensing of nitro-substituted compounds (Fig. 2).

Wang [9] and Li [10] et al. were able to obtain the porous networks Cu-UBTA and Cu-TUH based on the trigonal hexacarboxyl linkers H_6UBTA and H_6TUH (Fig. 3) with urea groups in the main chain and Cu^{2+} as a metal with a high adsorption capacity for CO_2 (165 $cm^3\ g^{-1}$ and 37 $cm^3\ g^{-1}$).

In this work, we introduce five new metal-organic networks of zinc, cadmium, and manganese with the linkers 4,4′-(carbonylbis(azanediyl))dibenzoate ($L1^{2-}$) and 4,4′-(carbonylbis(azanediyl))bis(3-methylbenzoate) ($L2^{2-}$) (Fig. 1). To the best of our knowledge this is the first report of single-ligand three-dimensional metal-

* Corresponding author.
E-mail addresses: janiak@hhu.de, janiak@uni-duesseldorf.de (C. Janiak).

https://doi.org/10.1016/j.ica.2017.09.029
0020-1693/

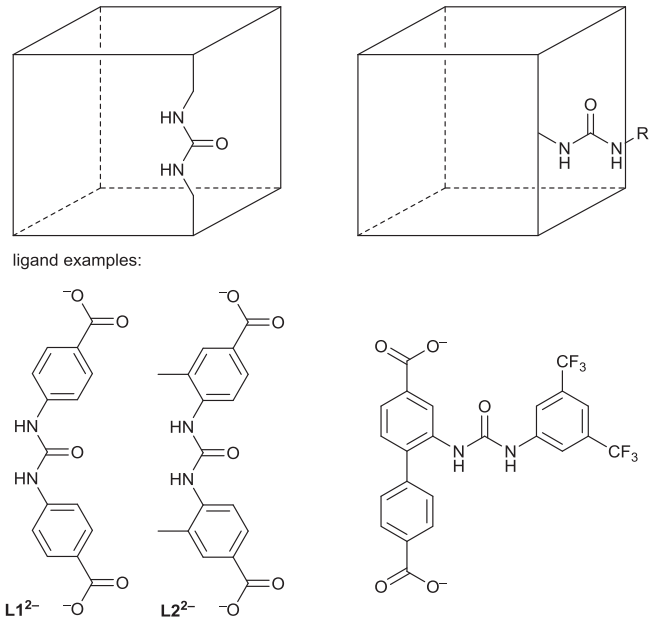

Fig. 1. Schematic presentation of possible positions of the urea function in dicarboxylate-linker MOFs. Left: Urea group in the main chain of the linker [8,12], right: in the side chain of a linker [8].

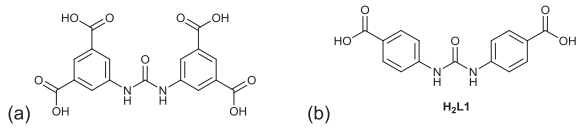

Fig. 2. The linker (as protonated forms) 5,5′-(carbonylbis(azanediyl))diisophthalic acid (a) for NU-601 [11] and 4,4′-(carbonylbis(azanediyl))dibenzoic acid (H_2L1, (b)) used for the syntheses TMU-18, -19 and -31 [8,12].

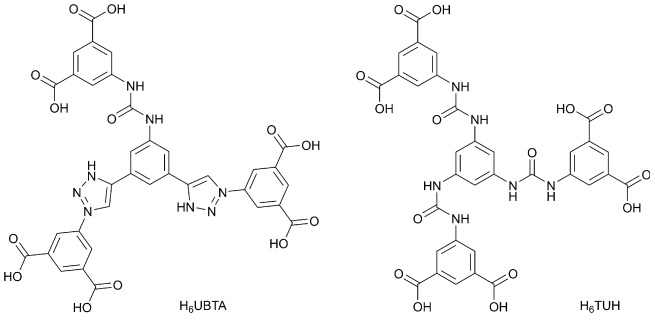

Fig. 3. Schematic presentation of the urea-functionalized linkers (protonated form) H_6UBTA and H_6TUH for the syntheses of the MOFs Cu-UBTA [9] and Cu-TUH [10].

organic networks constructed from a linear dicarboxylate linker with an urea group in the main chain, that is without co-ligands.

2. Results and discussion

2.1. Linker synthesis

The urea-containing ligands 4,4′-(carbonylbis(azanediyl)) dibenzoic acid (H_2L1) [17] and 4,4′-(carbonylbis(azanediyl))bis(3-methylbenzoic acid) (H_2L2) were synthesized in an one-step synthesis in a buffer system of aqueous boric acid and sodium hydroxide by the reaction of the aminobenzoic acid with triphosgene in THF (Scheme 1). Crystals of 4,4′-(carbonylbis(azanediyl))dibenzoic acid (H_2L1) were obtained by dissolving the ligand in a solution of

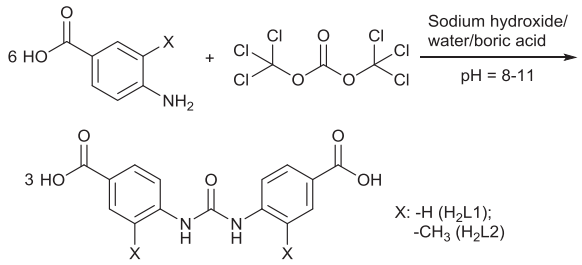

Scheme 1. Reaction scheme of the reaction of aminobenzoic acid with triphosgene in a buffer system of boric acid to the urea ligands H_2L1 and H_2L2.

water/ammonia, followed by slow evaporation of ammonia from the solution.

The thermal stability of both ligands H_2L1 and H_2L2 was investigated by thermogravimetric analysis (Fig. S1). Both ligands are stable up to 220 °C.

2.2. Metal-organic framework synthesis

The compounds **1**–**5** could be crystallized from the solvothermal reaction of the Linker H_2L1 or H_2L2 in DMF with different metal salts (Scheme 2). Due to the insolubility of the linkers in other solvents (H_2O, alcohols and nonpolar solvents) the crystallization processes were limited to basic, organic solvents like dimethylformamide, DMF. Compounds **1**, **2** and **5** were synthesized by reacting one equivalent of the metal nitrate salt with one equivalent of the dicarboxylic acid whereas crystals of compounds **3** and **4** were obtained with an excess of the metal salt in a molar ratio of 3:1 to the linker. Compound **4** can also be obtained by the reaction of $Zn(SO_4)\cdot 7\,H_2O$ as the metal salt source at 50 °C.

The infrared spectral bands for the carboxyl C=O vibrations for the linkers at 1420 cm^{-1} and 1377 cm^{-1} are shifted to lower wavenumbers upon metal compound formation which indicates the complete deprotonation of the linkers and the coordination at the metal centers.

For the example of compound **4**, the chemical stability during the activation process of the isoreticular compounds **3**–**5** was tested in more detail. The attempted exchange against other solvents ($CHCl_3$, EtOH and H_2O) yielded a white powder (investigated by PXRD, cf. Fig. S12 in Supp. Info.). For all compounds the crystals are stable in DMF and DMF can also be used as a washing solvent. Exposure to other solvents for solvent exchange as part of the attempted activation led to loss of crystallinity or to an undefinable

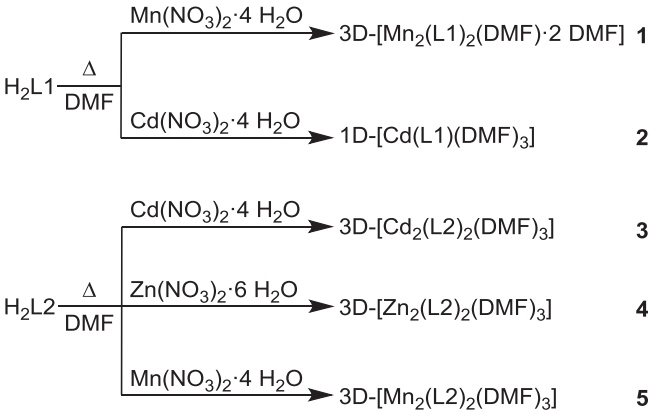

Scheme 2. Overview about synthesis and formulae of compounds **1**–**5**. Only the found and refined solvent molecules are given in the formulae. In the structures of compounds **1**, **3**–**5** the electron density contribution of additional solvent of crystallization was included in the recovered number of electrons in the voids by the SQUEEZE routine in PLATON [18].

crystalline state (cf. Fig. S12). Cadmium compound **3** was unstable in ambient air as indicated by powder X-ray diffraction (see below). For the analytical measurements the crystals of **3** were taken directly from the mother liquor and dried in a stream of dinitrogen to avoid degradation by air humidity. Attempted reaction of the linkers H_2L1 and H_2L2 with different metal salts ($Co(NO_3)_2$·6 H_2O, $Ni(NO_3)_2$·6 H_2O, $La(NO_3)_2$·6 H_2O) gave no crystalline products. The reaction with $Cu(NO_3)$·3 H_2O in different solvents (DMF, diethylformamide (DEF), dibutylformamide (DBF), dimethylacetamide (DMA)) gave microcrystalline plates whose structure could not be solved, however, and whose PXRD did not match with the known structures simulated from the single crystal structure of compounds **1**–**5**. For compound **4** the synthesis was also investigated in different solvents (DEF, DBF, DMA) but no crystals could be obtained.

Taking compound **4** as an example, the thermal stability was investigated by TGA under a continuous flow of nitrogen (Fig. S2). In the range up to 200 °C, the DMF solvent of crystallization as well the metal-coordinated DMF molecules (see below) are evaporated (theor. 30.4 wt% (see below), exp. 27.8 wt%). Following a short plateau around 200 °C, in the range between 200 °C and 300 °C, the coordinated three DMF molecules (theor. 15.2 wt%, exp. 12.6 wt%) are lost following by linker decomposition which is not finished at 600 °C. A ZnO residue would amount to only 5.6 wt% for a formula unit of $[Zn_2(L2)_2(DMF)_3]$·6DMF.

The unit cell void electron count of 1076 e in **4** can be tried to match to potential solvent molecules according to $Z \times \Sigma i$(solvent molecule i electron count × number of solvent molecules i in formula unit). With the DMF (C_3H_7NO) electron count of 40 e this gives an estimated 6 DMF molecules per formula unit in **4** ($Z = 4$). In the resulting formula unit of $[Zn_2(L2)_2(DMF)_3]$·6DMF ($C_{43}H_{49}N_7O_{13}Zn_2$·6($C_3H_7NO$)) with M = 1441.3 g/mol the six DMF crystal solvent molecules would amount to 30.4 wt%, the three coordinated DMF molecules to 15.2 wt%.

2.3. Crystal structures

2.3.1. Crystal structure of H_2L1

The asymmetric unit of the structure of the ligand 4,4′-(carbonylbis(azanediyl))dibenzoic acid, H_2L1 consists of half of the ligand molecule with a twofold axis passing through the urea C═O bond (Fig. 4a). The carboxylic acids are nearly coplanar to their aryl rings with dihedral angles of ~6°. The plane of the urea group is twisted to the planes of the adjacent aryl rings each by 45 °. Consequently both carboxylic acid groups and aryl rings assume dihedral angles of 71.3(1)° and 82.5(1)°, respectively.

The supramolecular crystal packing in the structure of H_2L1 is organized by classic O—H···O and N—H···O hydrogen bonds. The –COOH groups form tail-to-tail hydrogen bonds of the $R_2^2(8)$ motif in the Etter-notation (Fig. 4b) [19]. The urea N—H groups adopt the anti-relationship to their carbonyl group and form the expected three-center bond to the urea carbonyl group of an adjacent molecule with the C(4)[$R_2^1(6)$] motif (Fig. 4b) [19].

These strong H-bond interactions explain the low solubility of carboxylic acid/urea-molecules in water and in most common organic solvents. Dissolution of H_2L1 is only possible in basic solvent mixtures like dimethylformamide (DMF)/dimethylsulfoxide (DMSO)/dimethylacetamide (DMA) and in a pH-basic water solution, where it is possible to dissociate the H-bonds between the carboxylic acids by deprotonation in order to dissolve the molecule.

2.3.2. Crystal structure of compound 3D-[$Mn_2(L1)_2(DMF)$]·2 DMF (**1**)

Colorless crystals were obtained by the reaction of H_2L1 and manganese(II)-nitrate tetrahydrate in DMF after 24 days at a temperature of 105 °C. Compound **1** crystallizes in the triclinic crystal system with the space group *P*1. The asymmetric unit of **1** consists of two deprotonated $L1^{2-}$ ligands, two manganese atoms and three molecules of dimethylformamide. One dimethylformamide molecule is coordinated to the Mn2 atom, the other two molecules are connected via H-bonds to the hydrogen atoms of the urea group. However, only the O and C atom of this coordinated DMF solvent could be found and refined. The remaining $N(CH_3)_2$ part of the molecule was not found and is included in the recovered number of electrons in the void using the SQUEEZE routine in PLATON [18]. The coordination sphere is a distorted square pyramid for Mn1 and a distorted octahedron for Mn2 (Fig. 5).

The Mn1 atom is coordinated by five oxygen atoms from the carboxylate groups from five different L1 ligands. Two oxygen atoms O1 bridge between two Mn1 atoms in a rhombic Mn(μ–O)$_2$-

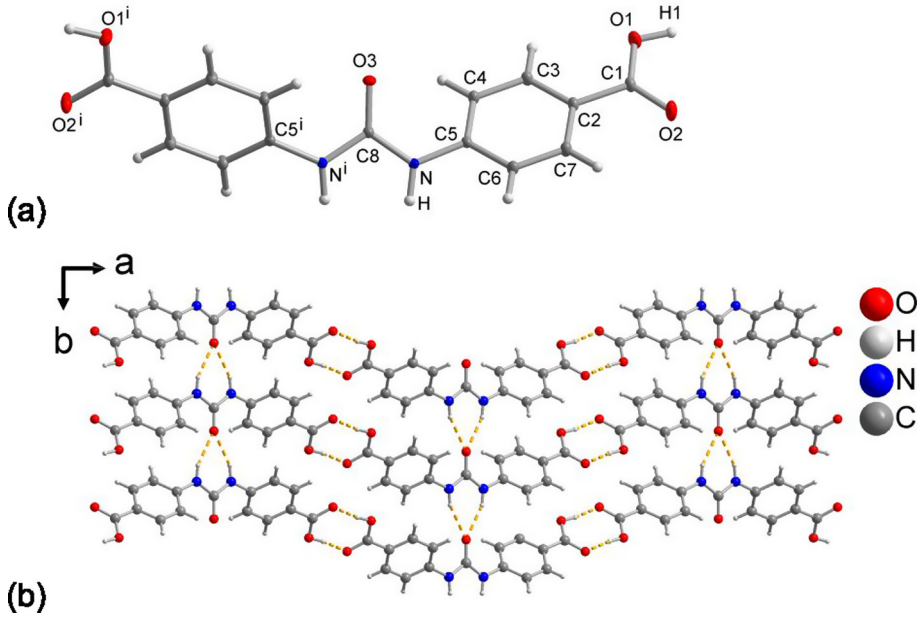

Fig. 4. a) Extended asymmetric unit of H_2L1 (50% thermal ellipsoids, H atoms with arbitrary radii). b) Section of the packing diagram in the H_2L1 structure with strong O—H···O and N—H···O H-bonding interactions indicated as orange dashed lines, see Table S1 in Supp. Info. for details. Symmetry transformation: i = −x, y, 3/2 − z.

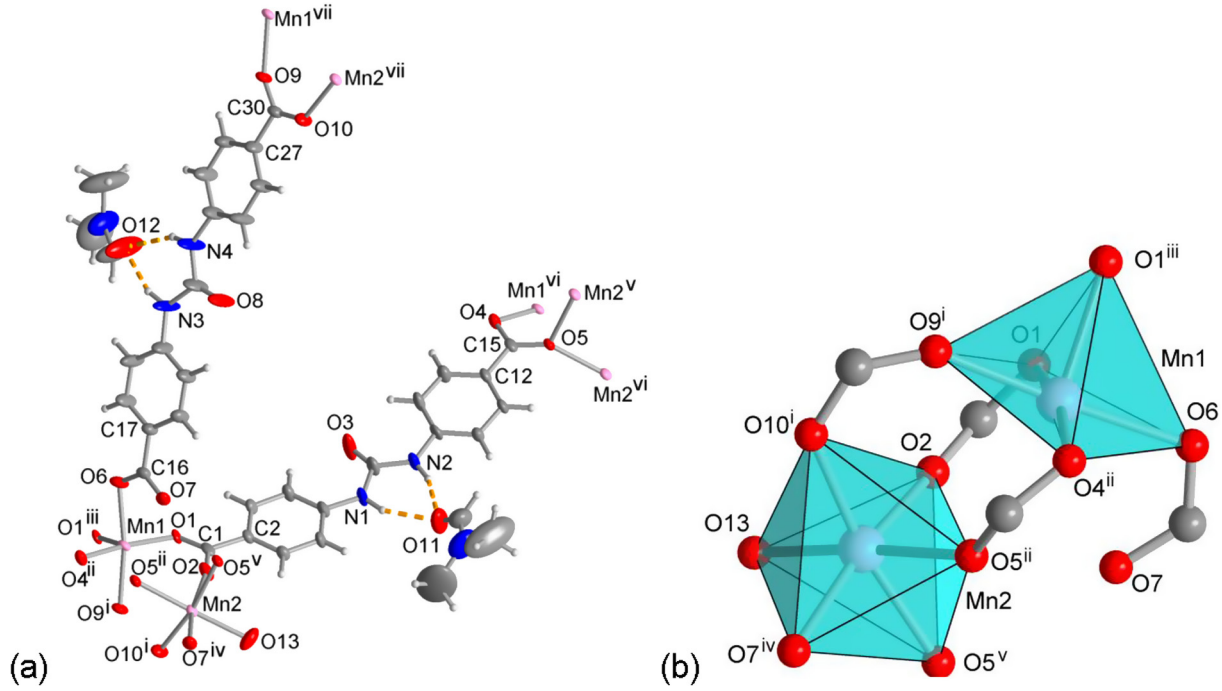

Fig. 5. Extended asymmetric unit of compound **1** (50% thermal ellipsoids) (a); polyhedra of the coordination environment of the two crystallographically different manganese atoms (b). Symmetry transformations: i = x, y + 1, z − 1; ii = x + 1, y, z − 1; iii = −x + 1, −y + 2, −z; iv = −x + 2, −y + 2, −z; v = −x + 1, −y + 2, −z + 1; vi = x − 1, y, z + 1; vii = x, y − 1, z + 1. Selected geometric parameters in Table S2 and S3, Supp. Info.

Mn fragment (Fig. 6a). The bond lengths for the Mn1-O bonds are in the range of 2.134–2.183 Å and the angles are between 78.44° and 113.34° for the oxygen atoms in cis-position and 168.03° and 171.64° for the atoms in trans-position.

The Mn2 atom is coordinated by five carboxylate oxygen atoms from five different L1 ligands and one oxygen atom of coordinated dimethylformamide. Two oxygen atoms O5 bridge between two Mn2 metal centers, forming again a rhombic $Mn(\mu{-}O)_2Mn$ fragment. The oxygen atom O5 is trans to the DMF ligand. The remaining three oxygen atoms belong to carboxylate groups which bridge as bidentate ligands between the metal atoms Mn1 and Mn2 (Fig. 6a). The bond lengths for the Mn2-O bonds are in the range from 2.100 Å (Mn2-O10^{i}) and 2.223 Å (Mn2-O5^{v}) and the angles are between 81.12° and 99.32° for the atoms in cis-position as well 166.18° and 175.76° for the atoms in trans-position.

The manganese-carboxylate substructures form one-dimensional chains parallel to the *a* direction (Fig. 6a) while the L1 ligands connect these metal-carboxylate chains in two other dimensions along the *b* and *b(−c)* direction to a three-dimensional network without any interpenetration (Fig. 6b). The network has infinite channels in the *a* direction, while the other two directions are blocked by the ligands. The channels have an opening of 4.6 × 19.6 Å along the diagonals of the parallelepiped cross-section (taking into account the van der Waals surface) (Fig. 6c).

*2.3.3. Crystal structure of compound 1D-[Cd(L1)(DMF)$_3$] (**2**)*

Colorless crystals were obtained by the reaction of H_2L1 and cadmium(II)-nitrate tetrahydrate in DMF. Compound **2** crystallizes in the monoclinic crystal system with the space group $P2_1/n$. The asymmetric unit of **2** consists of one cadmium atom, one ligand $L1^{2-}$ and three coordinated molecules of dimethylformamide at the cadmium atom (Fig. 7).

The cadmium atom is coordinated by seven oxygen atoms from which three below to coordinated dimethylformamide and four oxygen atoms are part of two different carboxylate groups of the $L1^{2-}$ ligand. Each carboxylate group coordinates in a bidentate chelating mode so that the ligand bridges between two Cd atoms. The coordination sphere for the central cadmium atom is pentagonal bipyramidal (Fig. 7b). The lengths of the cadmium-oxygen bonds are in the range between 2.297 Å and 2.425 Å and the angles in the range between 83.7° and 97.3° for the angles between the atoms in the axial and equatorial positions. The O–Cd–O angles between the *cis*-positioned O atoms in the equatorial plane are 54.9° and 55.2° for carboxylate chelate rings and 82.4° and 86.4° for the DMF O-atom to the carboxylate groups (Table S4).

The ligand and the cadmium atom form one-dimensional, linear chains where the distance between two cadmium atoms is 17.93 Å. The angle between two aryl rings from the ligand is 31.40° (Fig. 8). Parallel chains are arranged in double layers running either parallel to the *ab* axis or to the *(−a)b* axis (Fig. 8a). Chains running parallel to the different axes cross at an acute angle of 60°. Crossing chains are connected by N—H···O bonds (Fig. 8b, Table S5).

*2.3.4. Crystal structures of compounds 3D-[Cd$_2$(L2)$_2$(DMF)$_3$] (**3**), 3D-[Zn$_2$(L2)$_2$(DMF)$_3$] (**4**) and 3D-[Mn$_2$(L2)$_2$(DMF)$_3$] (**5**)*

Compounds **3**, **4** and **5** are isoreticular albeit not fully isotypic or isostructural as the space group of the room-temperature structure **3** (orthorhombic $Pna2_1$) is different to the space group of the structure **4** and **5** (monoclinic $P2_1/n$). However, the asymmetric unit, secondary building unit and network topology including the four-fold interpenetration of all three structures is identical (see below). Hence, we present and discuss here the structure of **3** as the example to the structures of **3**–**5**.

The asymmetric unit of **3** (Fig. 9) consists of two crystallographically different urea ligands $L2^{2-}$ and two cadmium atoms as well three dimethylformamide molecules coordinated to Cd1. From these three DMF ligands only the oxygen donor atoms (O11, O12 and O13) could be found and refined. The remaining –CH–N $(CH_3)_2$ part of the DMF ligand was strongly disordered and, hence, was included together with the non-coordinated solvent molecules in the recovered number of electrons in the void using the SQUEEZE routine in PLATON [18]. There are four formula units in the unit cell (Z = 4).

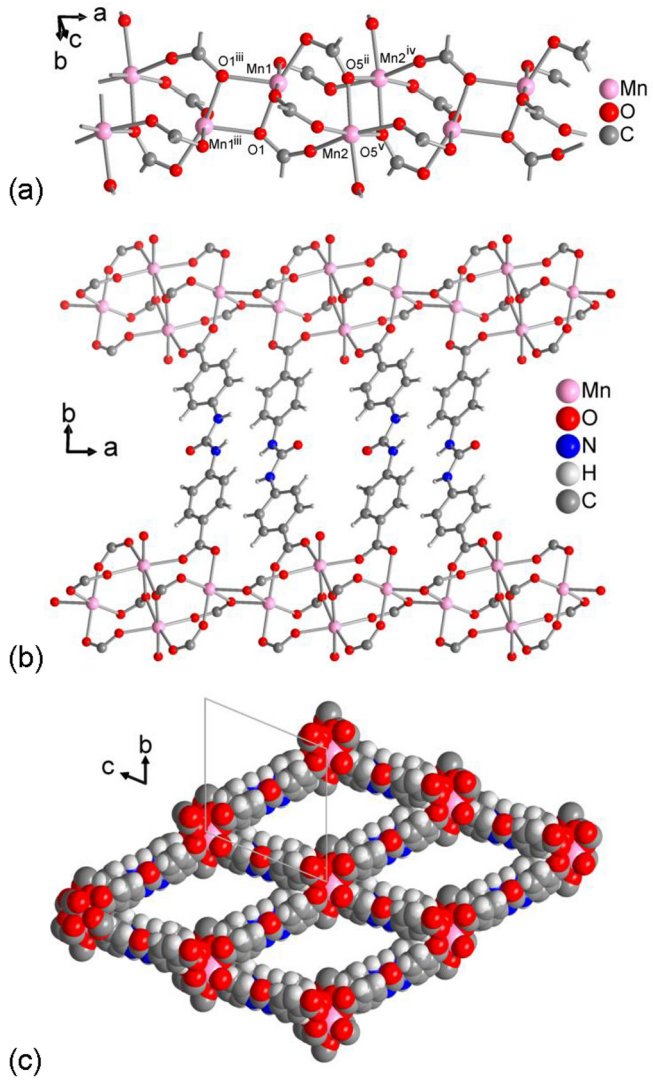

Fig. 6. (a) Infinite one-dimensional chain formed by the manganese atoms and the deprotonated carboxylic acids in **1**. (b) and (c) Sections of the packing diagram of **1**, with (b) view along the *c*-axis, and (b) along the *a* axis looking down the channels of the network (space-filling model with unit cell outline).

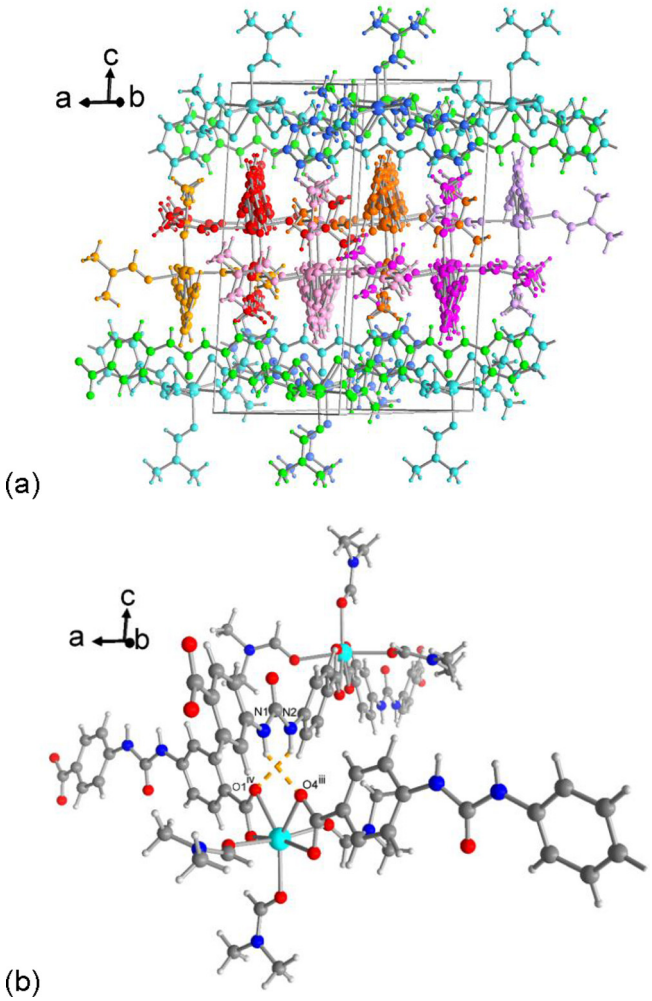

Fig. 8. (a) Section of the packing diagram in **2** with the different chains indicated by different color. Yellow-red-pink colors indicate chains running along the *ab* axis. Blue-green colors indicate chains running along the *(−a)b* direction. (b) Connection of crossing chains by N—H···O bonds (orange dashed lines) (details in Table S5, Supp. Info.).

Both cadmiums atoms Cd1 and Cd2 are coordinated by six oxygen atoms, each. The coordination sphere of Cd1 still appears as a rather regular octahedron in O–Cd–O bond angles (deviation less than 5.5° from 90°) but has different Cd-O bond distances (range 2.172–2.414 Å) (Table S6). The coordination sphere of Cd2 is distorted due to two chelating carboxylate groups with distances between 2.139 Å (Cd2-O2) and 2.627 Å (Cd2-O9) and angles

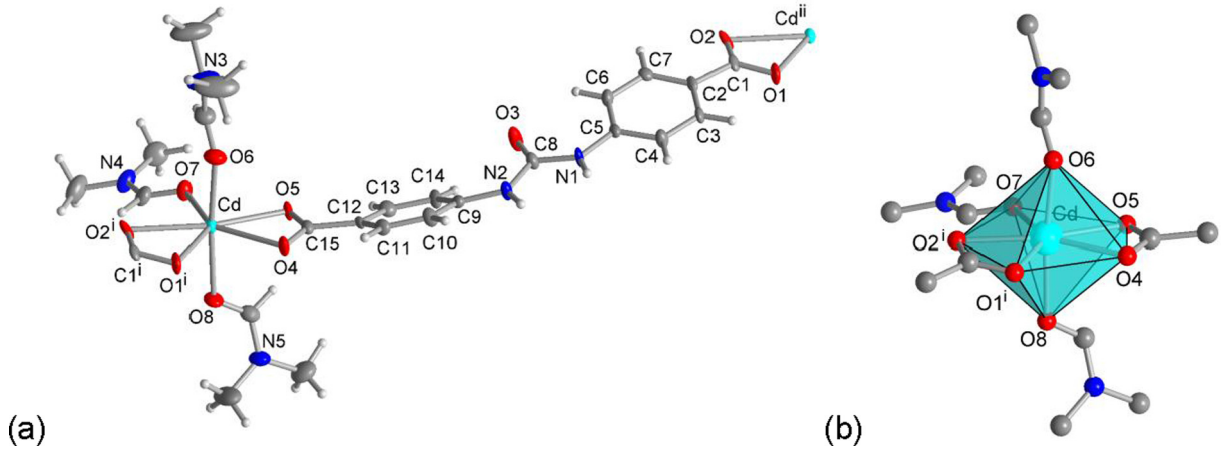

Fig. 7. (a) Asymmetric unit of compound **2** (50% thermal ellipsoids); (b) pentagonal-bipyramidal coordination sphere of the central cadmium atom in **2** with the three dimethylformamide ligands. Symmetry transformations: i = −1 + x, −1 + y, z; ii = 1 + x, 1 + y, z. Selected geometric parameters in Table S4, Supp. Info.

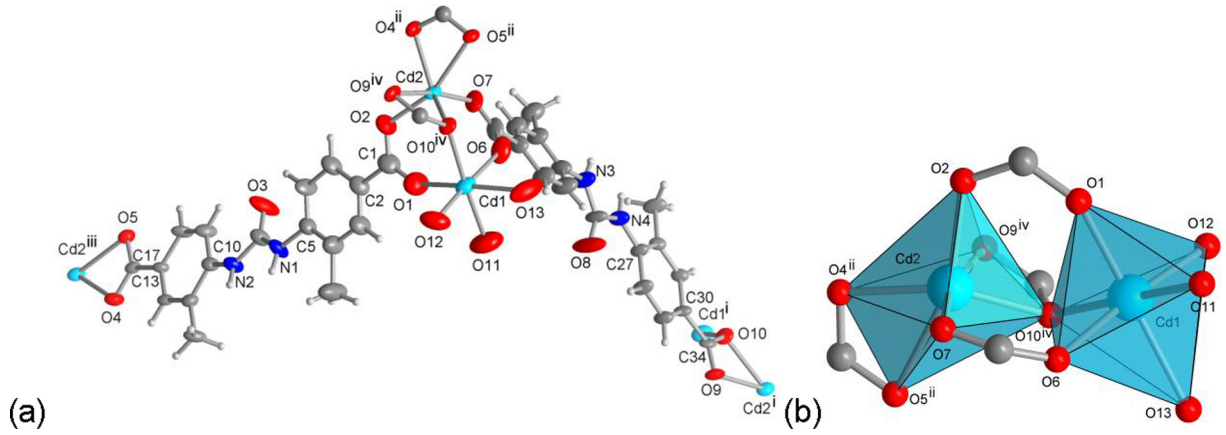

Fig. 9. (a) Extended asymmetric unit of compound **3** (30% thermal ellipsoids, room temperature structure). (b) Coordination polyhedra of the cadmium atoms. Oxygen atoms O11, O12, O13 are the donor atoms of three strongly disordered (hence 'squeezed') DMF ligands. Symmetry transformations: i = 3/2 − x, 1/2 + y, 1/2 + z; ii = 1/2 − x, −1/2 + y, 1/2 + z; iii = 1/2 − x, 1/2 + y, −1/2 + z; iv = 3/2 − x, −1/2 + y, −1/2 + z. Selected geometric parameters in Table S6, Supp. Info. See Figs. S5 and S6 for the corresponding asymmetric units of compounds **4** and **5**, respectively.

between 52.6° (O9-Cd2-O10) and 168.4° (O7-Cd2-O9), giving a more trigonal-prismatic coordination polyhedron [20–22] (Table S6, Fig. 9b). Both cadmium atoms are bridged by three carboxylate groups, with two of them bridging bis-monodentate (κ*O*:*O*') and one is chelating and bridging (κ*O*,*O*':*O*') (Fig. 12b). In addition, Cd1 is coordinated by three DMF solvent ligands, Cd2 is coordinated by a chelating bidentate carboxylate group from a bridging $L2^{2-}$ ligand. The secondary building unit in **3** can be ascribed as $\{Cd_2(O_2C-)_4\}$ with the four carboxylate carbon atoms at the vertices of a flattened and distorted tetrahedron with near C_{2v} symmetry (Fig. 10a). Overall, the $L2^{2-}$ ligand with the carboxylate oxygen atoms O1-O5 bridges between three cadmium atoms, the ligand with O6-O10 bridges between four cadmium atoms.

Thereby, the Cd atoms and the ligand form a three-dimensional network of diamondoid (6,6), **dia**-topology [23] topology (Fig. 10b). The 3 D network has large openings as channels in different directions. The node separation between the $\{Cd_2(O_2C-)_4\}$ SBUs of 17.6 Å and 19.7 Å gives rise to large voids in a single 3D network (Fig. 10b). Thus, four symmetry-related nets interpenetrate (Fig. 11) [24,25]. The individual networks in this fourfold interpenetrated structure are organized via H-bonds in the $C(4)[R_2^1(6)]$ motif [19] from the urea group to the carboxylate oxygen atoms O5 or O9 (Fig. 12, Table 2). Oxygen atoms O5 and O9 are the weakly coordinated donor atoms of the chelating carboxylate groups to Cd2, that is, have the longest Cd2-O bond distance (Table S7). Examples of porous MOF structures with fourfold interpenetration appear rare: 3D-$[Cu(I)_3(4,4'\text{-bipy})_5]_2[H_2SiW_{11}O_{39}]\cdot 5H_2O$ (4,4'-bipy = bipyridine) [26], the diamondoid network $[Co(pybz)_2]\cdot 2$ DMF ($pybz^-$ = 4-(4-pyridyl) benzoate anion) in which the DMF crystal solvent can be removed from the channels to give a potentially porous framework that however shows no N_2-uptake [27]; the diamondoid MOF $\{[Ni_4(44pba)_8]\cdot sol\}_n$, (44pba = 4-(4-pyridyl)benzoate), which was investigated for the adsorption of a wide range of solvents like methanol, ethanol, benzene or dimethylformamide [28] and the diamondoid network $([Zn_4O\{Cu(L)_2\}_2]$ (L = bis(N-heterocyclic) complex) [29]. Thus, a fourfold interpenetration seems to correlate closely with **dia** network topology.

The fourfold interpenetrated networks in **3**–**5** still have open channels, primarily in the *a*-direction. The channels provide a solvent accessible volume of about 50% of the total unit cell volume (cf. Table 1). The electron density coming from disordered DMF solvent in these voids was recovered by the SQUEEZE option in PLATON [18].

To the best of our knowledge, compounds **1** and **3**–**5** are the first three-dimensional networks with an urea group in the main chain of the ligand and without an additional co-linker like 4,4'-bipyridin [30]. Although other groups have also attempted to get crystal structures with the ligand H_2L1 no single-ligand network structure is known in the literature with this ligand [13].

Powder X-ray diffractometry (PXRD) confirmed the reproducible synthesis (Fig. S11, Supp. Info.), phase purity and representative nature of the single crystals. For the representative nature and phase purity it is crucial to be aware that the simulated diffractograms were derived from crystal data where the considerable amount of solvent-derived electron density in the voids had been removed by the SQUEEZE option in PLATON [18]. In structure **1** and **3**–**5** also part of the coordinated DMF ligands were included in SQUEEZE because of unrefinable disorder. Even if the DMF crystal solvent in the voids is disordered its electron density still contributes to diffraction. Hence, the experimental diffractograms of the as-synthesized samples differ in their intensities (Figs. S9 and S10, Supp. Info.). In the case of sample **4** a single-crystal data set before SQUEEZE was refined to the stage where most of the solvent electron density was assigned to individual atoms. Consequently, the simulated diffractogram now gave a better match to the PXRD of the as-synthesized sample (Fig. S10, Supp. Info.).

Powder X-ray diffractometry also showed that the crystallinity of the samples started to get lost when kept in ambient air for 24 h (Fig. S9) and when the DMF solvent was tried to exchange against ethanol or chloroform or when the samples were dried under vacuum as part of the activation procedure before gas sorption studies (Fig. S12 in Supp. Info.).

For the measurement of the N_2-adsorption isotherm at 77 K, the as-synthesized sample of **4** was degassed for 12 h at 120 °C under continuous vacuum. After the activation, loss of crystallinity possibly with a change in the structure of the compound was observed by PXRD (Fig. S12). For the activated sample of **4**, no nitrogen uptake was seen; hence no BET-surface area could be determined.

Also a dye sorption experiment did not confirm the potential porosity. As-synthesized crystals of compound **4** (2 mg) were added to a solution of methylene blue (MB) in DMF (c = 0.02 g/L) in a cuvette. The UV–Vis absorption was measured immediately after the addition and again after 24 h. Neither spectrometrically (Fig. S13a in Supp. Info.) nor visually (Fig. S13b) could a change in absorption intensity be observed. The crystals of compound **4** remained colorless.

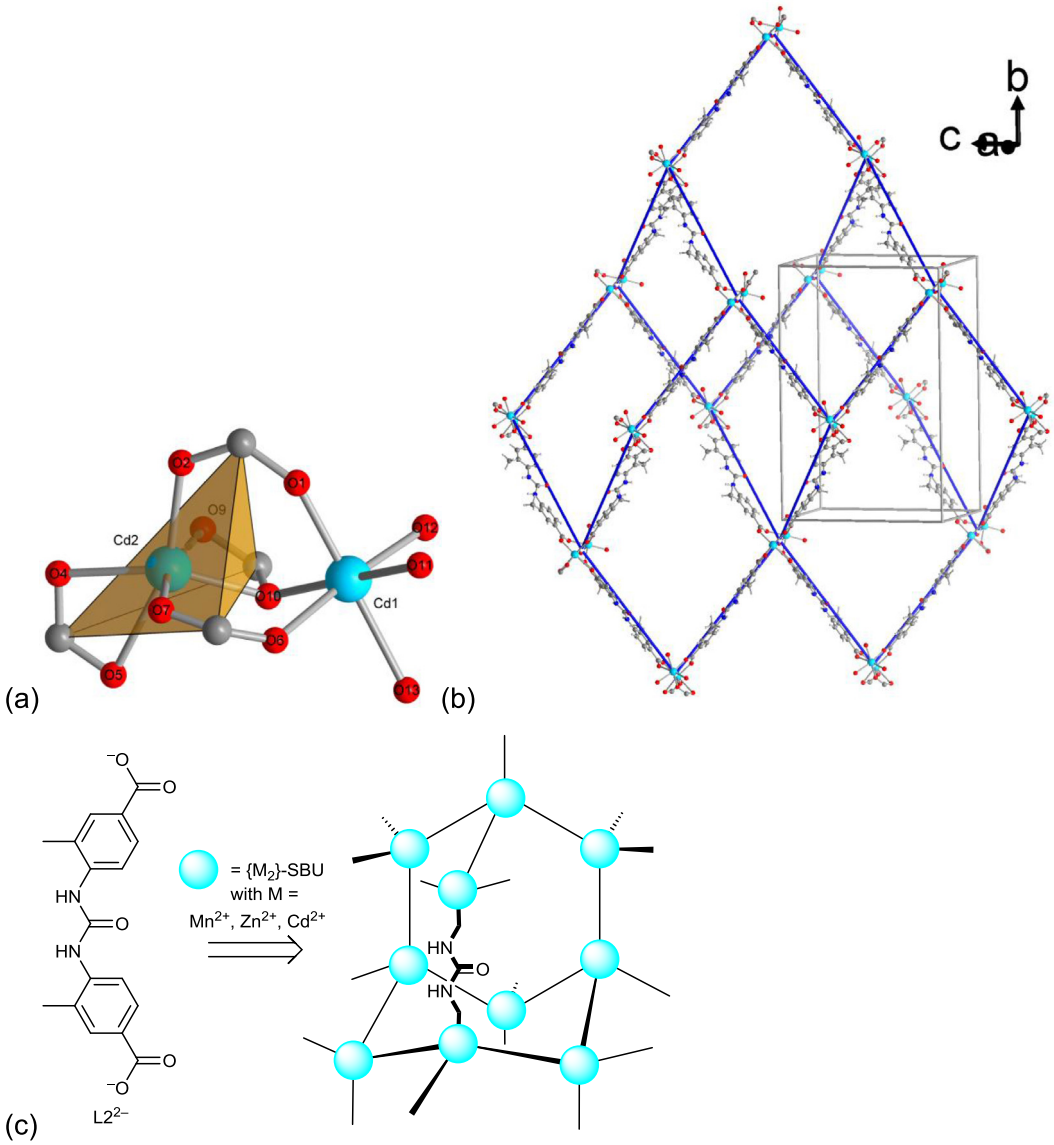

Fig. 10. (a) Secondary building unit (SBU) $\{Cd_2(O_2C-)_4\}$ showing the four carboxylate carbon atoms as the vertices of a flattened and distorted tetrahedron from which (b) the 3D network of diamondoid (**dia**) topology originates. Three adamantane cages of the **dia** network are depicted in (b) together with the SBU centroid connections as dark blue lines and the unit cell outline of **3** (identical in **4** and **5**). (c) Schematic representation of the diamondoid network with the ligand $L2^{2-}$.

3. Experimental section

3.1. Materials and methods

The chemicals used were obtained from commercial sources and no further purification has been carried out. For aqueous solutions doubly de-ionized water was used. Organic solvents were of reagent grade and dried over molar sieve. The ligands were synthesized starting from the aminobenzoic acids in a one-step-synthesis. CHN analysis was performed with a Perkin Elmer CHN 2400. Fourier-transform infrared (FT-IR)-spectra were recorded on a Bruker Tensor 37 IR spectrometer as KBr pellet or with attenuated total reflection (ATR) unit (Platinum ATR-QL, Diamond). The intensity of absorption is indicated as strong (s), medium (m), weak (w) and broad (br). Thermogravimetric analysis (TGA) was done with a Netzsch TG 209 F3 Tarsus in the range from 20 to 600 °C, equipped with Al-crucible and applying a heating rate of 3 K min^{-1} under inert atmosphere (N_2). Prior to measurement, the MOF sample was exposed to a continuous stream of nitrogen in an open Schlenk tube for one hour to remove any outer-surface solvent molecules. Powder X-ray diffractograms (PXRDs) were measured on a Bruker D2 Phaser with a flat silicon, low background sample holder, at 30 kV, 10 mA, a scan speed of 0.2 s/step and a step size of 0.02° (2θ) with Cu-K ψ radiation (λψ = 1.5418 Å). In all diffractograms, the most intensive reflection was normalized to 1. NMR spectra were measured with a Bruker Avance DRX-600 spectrometer. Electron-spray ionization mass spectra (ESI-MS) were collected with a UHR-QTOF maXis 4G from Bruker Daltonics.

3.2. Syntheses

3.2.1. Synthesis of 4,4′-(carbonylbis(azanediyl))dibenzoic acid ($C_{15}H_{12}N_2O_5$, H_2L1)

H_2L1 has been described in the literature with a multistep synthesis [17]. Here H_2L1 has been synthesized different to the known literature procedure with the reagent triphosgene, which is highly selective for amide formation from amino groups. Therefore no additional protection of the carboxylic acid was needed for the following synthesis [31].

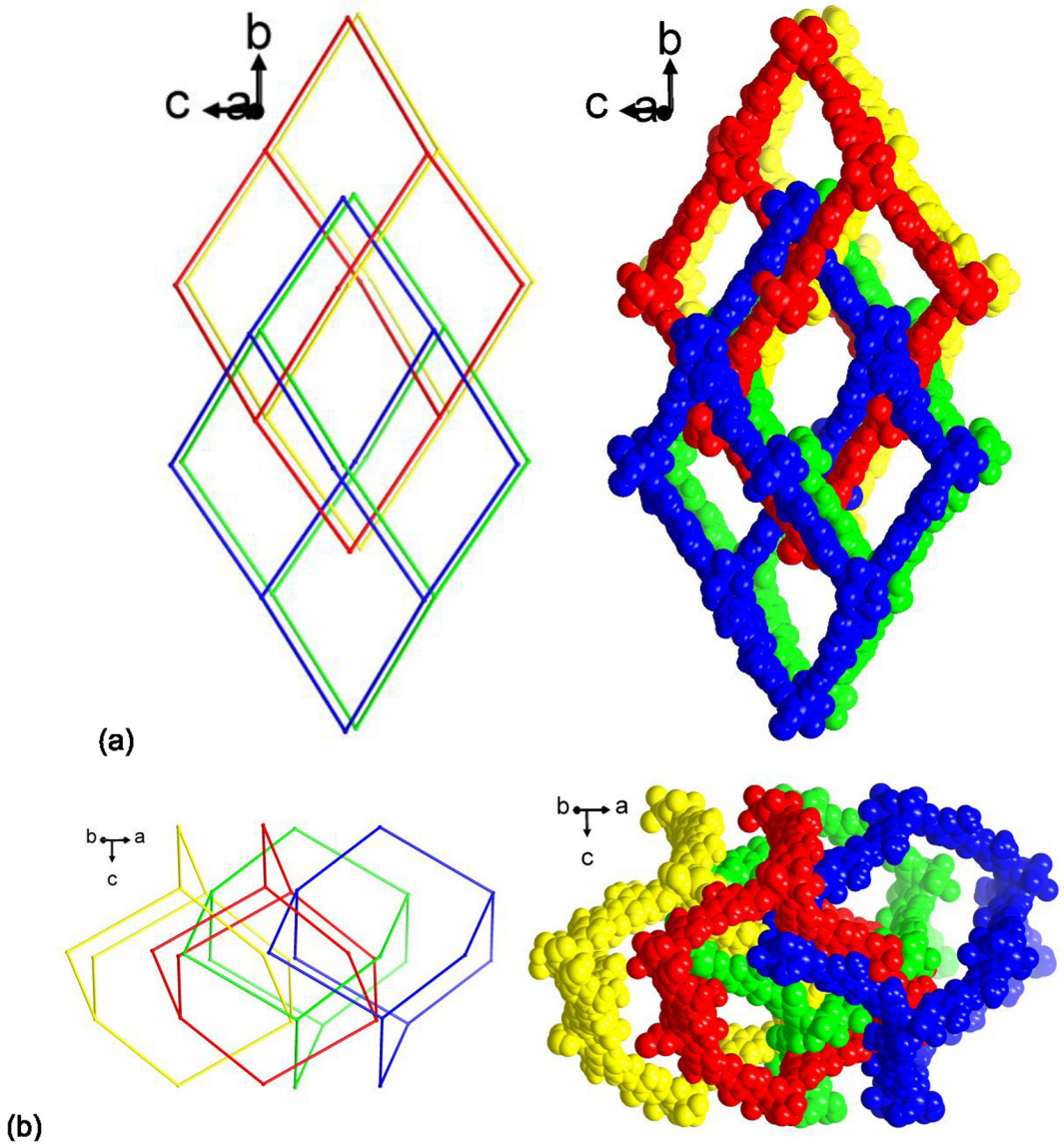

Fig. 11. Section of the fourfold interpenetrated symmetry-related networks in compound **3** (identical in **4** and **5**) with each network represented by a single adamantane cage in different color. The space-filling mode illustrates that despite the interpenetration a potential porosity (~50% solvent-filled void space of unit-cell volume) is retained in **3**–**5**. View approximately along (a) *a* axis, (b) *ab* axis.

4-Aminobenzoic acid ($C_7H_7NO_2$, 1.65 g, 12.0 mmol), boric acid (H_3BO_3, 43.2 mmol, 2.67 g) and sodium hydroxide (NaOH, 33.6 mmol, 1.32 g) were dissolved in water (150 mL) to obtain a buffer solution with a pH of ~9. To this, a solution of triphosgene ($C_3Cl_6O_3$, 3.00 mmol, 0.89 g) in THF (20 mL) was added over a period of 30 min. The solution was stirred for 10 additional minutes and conc. HCl (2 mL) was added. The withe precipitate was filtered off (pore 4 filter) and washed with water (2 × 50 mL) and once with THF (50 mL). The white solid was dried under vacuum for 4 h at 120 °C. Yield: 1.26 g (4.19 mmol, 70% based on 4-aminobenzoic acid).

Crystals of H_2L1 were obtained by suspending H_2L1 in water and dissolving it by adding a few drops of aqueous ammonia solution. By slow evaporation of the ammonia, single crystals were obtained after about 3 weeks.

FT-IR (KBr, cm^{-1}): 3321 (m), 3185 (w), 3074 (w), 2983 (w), 2831 (w), 2669 (w), 2554 (w), 2362 (w), 1666 (s), 1596 (m), 1539 (s), 1420 (m), 1305 (s), 1224 (m), 1176 (m), 1120 (w), 935 (w), 864 (w), 760 (m), 651 (w), 608 (w), 547 (w), 510 (w).

^{1}H-NMR (300 MHz, DMSO-d_6, ppm): δ = 12.63 (s, 1 H), 9.15 (s, 1 H), 7.88 (d, *J* = 8.8 Hz, 2 H), 7.58 (d, *J* = 8.8 Hz, 2 H).

^{13}C{^{1}H}-NMR (300 MHz, DMSO-d_6): δ = 167.35, 152.31, 144.00, 130.91, 124.37, 117.81.MS (ESI[+]): *m*/*z* = 301.1 $[M + H]^+$ (calc.: 301.1).

Elemental analysis ($C_{15}H_{12}N_2O_5$, 300.27): calc. C 60.00, H 4.03, N 9.33%; found C 59.82, H 4.08, N 9.14%.

3.2.2. Synthesis of 4,4′-(carbonylbis(azanediyl))bis(3-methylbenzoic acid) ($C_{17}H_{16}N_2O_5$, H_2L2)

4-Amino-3-methylbenzoic acid ($C_8H_9NO_2$, 1.81 g, 12.00 mmol), boric acid (H_3BO_3, 43.20 mmol, 2.67 g) and sodium hydroxide (NaOH, 33.00 mmol, 1.32 g) were dissolved in water (150 mL) as a buffer system with a pH of ~9. To this a solution of triphosgene ($C_3Cl_6O_3$, 3.00 mmol, 0.89 g) in THF (20 mL) was added over a period of 30 minutes. The solution was stirred for 10 additional minutes and conc. HCl (2 mL) was added. The withe precipitate was filtered off (pore 4 filter) and washed two times with water (2 × 50 mL) and once with THF (50 mL). The white solid was dried

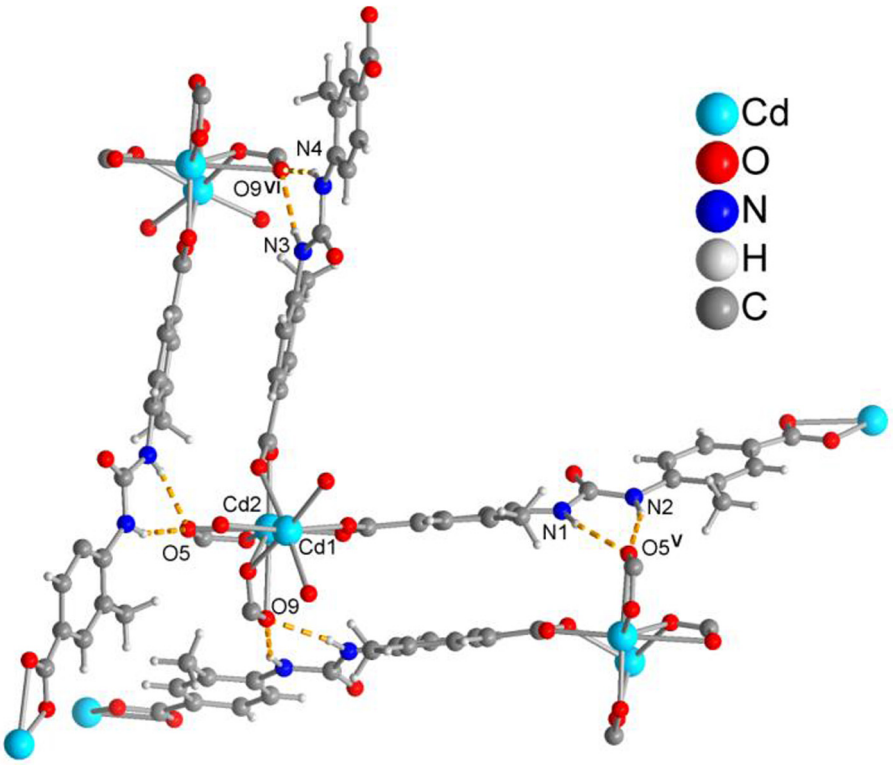

Fig. 12. Connection of symmetry related networks by N—H···O bonds (orange dashed lines) in compound **3** (identical in **4** and **5**) (details in Table S7, S9 and S12, respectively, Supp. Info.).

for 18 h at 80 °C. Yield: 1.38 g (4.19 mmol, 70% based on 4-amino-3-methylbenzoic acid). FT-IR (KBr, cm^{-1}): 3281 (m), 2971 (m), 1696 (s), 1637 (s), 1587 (m), 1547 (s), 1429 (m), 1308 (m), 1271 (m), 1184 (m), 1127 (w), 937 (w), 977 (w), 837 (w), 764 (m), 656 (w), 563 (w).

^{1}H-NMR (300 MHz, DMSO-d_6, ppm): δ = 12.61 (s, 1 H), 8.67 (s, 1 H), 8.09 (d, *J*=8.5 Hz, 1 H), 7.84–7.67 (m, 2 H), 2.34 (s, 3 H).

^{13}C{^{1}H}-NMR (300 MHz, DMSO-d_6, ppm): δ = 167.15, 152.23, 141.68, 131.52, 127.86, 126.57, 124.29, 119.62, 18.13.

MS (ESI[+]): *m*/*z* = 329.3 $[M + H]^+$ (calc.: 329.3).

Elemental analysis ($C_{17}H_{16}N_2O_5$, 328.32): calc. C 62.19, H 4.91, N 8.53%; found C 62.09, H 4.84, N 8.25%.

3.2.3. Synthesis of $[Mn_2(L1)_2(DMF)]\cdot 2\,DMF$ (**1**)

In a DURAN glass vial, $Mn(NO_3)_2\cdot 4H_2O$ (5.0 mg, 20 µmol) and H_2L1 (6.0 mg, 20 µmol) were dissolved in DMF (2.5 mL). The vial was sealed, sonicated in an ultrasound bath for 10 min and the crystals were allowed to grow at a temperature of 105 °C for 24 days. After this time, a small amount of colorless crystals had formed (yield ~1.2 mg, 7%) together with a brownish precipitate of MnO_2. An attempted scale-up of this procedure resulted only in a white powder but no crystals anymore.

FT-IR (ATR, cm^{-1}): 3344 (w), 3301 (w), 1712 (w), 1647 (m), 1599 (m), 1571 (m), 1526 (m), 1385 (s), 1307 (m), 1233 (m), 1200 (m), 1172 (s), 1102 (m), 1061 (w), 1013 (w), 900 (w), 860 (m), 782 (m), 701 (w), 664 (m), 635 (w), 618 (m), 567 (w).

3.2.4. Synthesis of $[Cd(L1)(DMF)_3]$ (**2**)

In a DURAN glass vial, $Cd(NO_3)_2\cdot 4H_2O$ (6.1 mg, 20 µmol) and **H_2L1** (6.0 mg, 20 µmol) were dissolved in DMF (2.5 mL). The vial was sealed, sonicated in an ultrasound bath for 10 min and the crystals were allowed to grow at a temperature of 105 °C for 14 days. After this time, colorless crystals had formed (yield ~1.5 mg, 24%).

FT-IR (ATR, cm^{-1}): 3284 (w), 2931 (w), 1705 (w), 1638 (s), 1598 (s), 1557 (m), 1507 (m), 1436 (w), 1391 (s), 1304 (s), 1238 (m), 1210 (m), 1171 (s), 1141 (w), 1103 (m), 1061 (w), 1035 (w), 900 (w), 860 (m), 832 (w), 783 (s), 750 (w), 702 (w), 672 (m), 621 (m).

3.2.5. Synthesis of $[Cd_2(L2)_2(DMF)_3]$ (**3**)

In a DURAN glass vial, $Cd(NO_3)_2\cdot 4H_2O$ (18.4 mg, 60 µmol) and **H_2L2** (6.6 mg, 20 µmol) were dissolved in DMF (5.0 mL). The vial was sealed, sonicated in an ultrasound bath for 10 min and the crystals were allowed to grow at a temperature of 80 °C for 5 days. After this time, colorless cubic crystals were collected (Fig. S3), (yield ~1.4 mg, 8%).

FT-IR (ATR, cm^{-1}): 3281 (m), 1641 (m), 1594 (m), 1559 (m), 1517 (s), 1492 (m), 1406 (s), 1391 (s), 1308 (m), 1278 (m), 1258 (m), 1224 (w), 1192 (m), 1139 (m), 1112 (m), 1051 (w), 1036 (w), 1005 (w), 924 (w), 918 (w), 886 (w), 856 (w), 843 (w), 823 (m), 777 (s), 747 (m), 714 (w), 672 (m), 633 (m), 568 (w).

3.2.6. Synthesis of $[Zn_2(L2)_2(DMF)_3]$ (**4**)

In a DURAN glass vial, $Zn(NO_3)_2\cdot 6H_2O$ (6.0 mg, 20 µmol) and H_2L2 (6.6 mg, 20 µmol) were dissolved in DMF (2.5 mL). The vial was sealed, sonicated in an ultrasound bath for 10 min and the crystals were allowed to grow at a temperature of 50 °C for 14 days. After several days, colorless cubic crystals were collected (yield ~8.0 mg, 42%) (Fig. S4). In contrast to the synthesis at 50 °C, the synthesis at 105 °C gives crystals of compound **4** after three days.

FT-IR (ATR, cm^{-1}): 3346 (m), 2924 (w), 1656 (s), 1623 (s), 1592 (s), 1526 (s), 1418 (s), 1382 (s), 1308 (m), 1269 (m), 1247 (m), 1205 (m), 1181 (m), 1136 (m), 1100 (m), 810 (s), 782 (m), 661 (w), 636 (w).

Table 1
Crystal data and structure refinement for compounds H_2L1 and **1**–**5**.

Compound	H_2L1	1	2
Chemical formula	$C_{15}H_{12}N_2O_5$	$C_{31}H_{20}Mn_2N_4O_{11}\cdot 2(C_3H_7NO)$[e]	$C_{24}H_{31}CdN_5O_8$[f]
M/g mol^{-1}	300.27	880.58	629.94
Crystal system, space group	Monoclinic, *C*2/*c*	Triclinic, *P*1	Monoclinic, $P2_1/n$
Temperature/K	140	150	100
a/Å	13.5100(11)	9.6545(6)	9.2718(7)
b/Å	4.7129(3)	17.2717(10)	15.3481(11)
c/Å	19.8387(16)	17.326(1)	19.9685(15)
α/°	90	66.504(3)	90.00
β/°	91.425(5)	77.105(4)	94.808(4)
γ/°	90	83.163(3)	90.00
V/Å^3	1262.76(17)	2581.3(3)	2831.6(4)
Z	4	2	4
D_{calc}/g cm^{-3}	1.579	1.133	1.478
μ (mm^{-1})	0.121	0.54	0.82
Crystal size (mm)	0.16 × 0.10 × 0.04	0.11 × 0.10 × 0.08	0.10 × 0.10 × 0.01
F(000)	624	904	1288
absorpt. correct. T_{min}, T_{max}	0.666, 0.753	0.669, 0.745	0.669, 0.745
Reflections collected, independent and observed [I > 2σ(I)]	20524, 2848, 2266	30330, 8159, 6118	9963, 5601, 4583
R_{int}	0.043	0.049	0.058
Data/parameters/restraints	2848/107/0	8159/527/0	5601/350/0
$(\sin\theta/\lambda)_{max}$ (Å^{-1})	–	0.58	0.619
$\Delta\rho_{max}$, $\Delta\rho_{min}$ (e Å^{-3})[a]	0.519, −0.402	0.63, −0.75	3.55, −2.58
R_1/wR_2 [I>2σ(I)][b]	0.0390/0.1123	0.0497/1380	0.0705/0.1492
R_1/wR_2 (all data)[b]	0.0521/0.1221	0.705/0.1505	0.0889/0.1553
Goodness-of-fit on F^2[c]	1.050	1.050	1.130
Void electron count/e[d]	–	351	–
Void, solvent accessible volume/Å^3 (% unit cell volume)[d]	–	826 (32%)	–

[a] Largest difference peak and hole.
[b] $R_1 = [\sum(||F_o| - |F_c||)/\sum|F_o|]$; $wR_2 = [\sum[w(F_o^2 - F_c^2)^2]/\sum[w(F_o^2)^2]]^{1/2}$.
[c] Goodness-of-fit = $[\sum[w(F_o^2 - F_c^2)^2]/(n-p)]^{1/2}$.
[d] Recovered number of electrons in the void, solvent accessible volume; both found by using the SQUEEZE routine in PLATON (probe radius 1.2 Å) [18]. The unit cell void electron count can be tried to match to potential solvent molecules according to $Z \times \Sigma i$(solvent molecule *i* electron count × number of solvent molecules *i* in formula unit). Electron count for solvent molecules *i*: DMF (C_3H_7NO) 40 e.
[e] Only the O and C atom of this coordinated DMF solvent could be found and refined. The remaining $N(CH_3)_2$ part of the molecule was not found and is included in the recovered number of electrons in the void using the SQUEEZE routine in PLATON [18].
[f] Refined as a 2-component twin, see text in Section 3.2.8.

Table 2
Crystal data and structure refinement for compounds H_2L1 and **1**–**5** (contd.).

3	4	5
$C_{34}H_{28}Cd_2N_4O_{13}$[g]	$C_{40}H_{42}N_6O_{13}Zn_2$ [h]	$C_{40}H_{42}Mn_2N_6O_{13}$[i]
925.4	945.53	924.67
Orthorhombic, $Pna2_1$[g]	Monoclinic, $P2_1/n$	Monoclinic, $P2_1/n$
293	100	100
14.730(3)	14.232(5)	14.571(5)
28.473(7)	20.366(7)	18.145(6)
18.577(5)	26.441(9)	28.255(9)
90.00	90.00	90.00
90.00	90.884(13)	91.663(7)
90.00	90.00	90.00
7791(3)	7663(5)	7467(4)
4	4	4
0.789	0.820	0.822
0.58	0.67	0.38
0.30 × 0.30 × 0.08	0.08 × 0.08 × 0.06	0.06 × 0.03 × 0.02
1840	1952	1908
0.590, 0.745	0.636, 0.744	–
71896, 7554, 6842	30835, 5698, 4501	9868, 2091, 1533
0.096	0.068	0.081
7554/483/427	5698/558/480	2091/252/0
0.493	0.450	0.324
2.00, −0.77	0.60, −0.66	0.44, −0.75
0.0487/0.1210	0.0983/0.2541	0.1201/0.3435
0.0547/0.1261	0.1177/0.2787	0.1473/0.3657
1.056	1.071	1.593
1113	1076	734
4798 (62%)	4245 (55%)	3921 (52%)

[g] In an attempted low-temperature data set different ligand conformations were frozen which lead to increased disorder so that the quality of refinement became even lower. Further, the structure of **3** in the non-centrosymmetric space group $Pna2_1$ was refined as an inversion twin with a Flack parameter of 0.48(4) [39]. From the three coordinated DMF molecules only the O donor atoms were found and refined.
[h] The atoms of two of the three metal-coordinated DMF ligands were found and refined. For the third coordinated DMF only the O donor atom was found and refined.
[i] Despite the low data quality the topology of the 3D metal-ligand network in **5** could be unequivocally determined, including the atoms of two of the three metal-coordinated DMF ligands. For the third coordinated DMF only the O donor atom was found and refined.

3.2.7. Synthesis of $[Mn_2(L2)_2(DMF)_3]$ (**5**)

In a DURAN glass vial, $Mn(NO_3)_2\cdot 4H_2O$ (5.0 mg, 20 μmol) and H_2L2 (6.6 mg, 20 μmol) were dissolved in DMF (2.5 mL). The vial was sealed, sonicated in an ultrasound bath for 10 min and the crystals were allowed to grow at a temperature of 105 °C for 11 days. After this time, a small amount of colorless crystals had formed (yield ~1.4 mg, 8%) together with a brownish precipitate of MnO_2. Only a low amount of small crystals were obtained. Due to the low yield, no powder diffractogram could be recorded.

FT-IR (KBr, cm^{-1}): 3345 (w), 3294 (w), 1700 (w), 1647 (m), 1616 (w), 1593 (m), 1518 (m), 1416 (m), 1379 (s), 1310 (m), 1273 (m), 1249 (m), 1209 (w), 1184 (m), 1141 (w), 1106 (m), 1004 (w), 940 (w), 910 (w), 808 (m), 779 (m), 664 (m), 634 (m).

3.2.8. Single crystal X-ray structures

Suitable crystals for measurement were carefully selected under a polarizing microscope, covered with protective oil and mounted on a glass loop. Unit cell parameters were determined by a least-squares fit of 2θ values and intensity data were measured on a Bruker Kappa DUO with APEX II CCD area detector equipped with microfocus sealed tube, Mo-Kα radiation (λ = 0.71073 Å) and multilayer mirror monochromator. Data collection by ω- and ϕ-scans with APEX II [32], cell refinement with SMART, data reduction with SAINT [33]. The intensities were corrected for empirical absorption based on multi-scan technique using the SADABS program [34]. *Structure analysis and refinement:* The structures were solved by direct methods and refined by full-matrix least-squares fitting on F^2 by SHELX 97 [35]. All non-hydrogen atoms were refined with anisotropic thermal parameters, except in the structure of **5** which was only refined isotropically due to low number of data. Hydrogen atoms were

positioned geometrically and refined using riding models [AFIX 43 for aromatic CH with C—H = 0.95 Å, $U_{iso}(H) = 1.2U_{eq}(C)$, AFIX 137 for CH_3 with C—H = 0.98 Å and $U_{iso}(H) = 1.5U_{eq}(C)$]. The hydrogen atoms on the urea nitrogen atoms were positioned geometrically (N—H = 0.88 Å) and refined using a riding model (AFIX 43) with $U_{iso}(H) = 1.2U_{eq}(N)$. In the structure of the ligand H_2L1 he N—H and carboxyl O—H atoms have been found and refined with $U_{iso}(H) = 1.5U_{eq}(N,O)$.

Crystallographic data are summarized in Table 1. For the X-ray structure analyses of the metal compounds **1**–**5** we picked the largest crystals we could locate in the compounds. Even these were mostly of very small size (cf. Table 1). It is known that very small crystals diffract weaker than larger crystals, resulting in lower data quality and subsequent problems during refinement [36]. Some of the checkcif alerts are due to the small crystal size, e.g., poor data/-parameter ratio. For each compound **1**–**5** two to three crystals each were mounted on the diffractometer and data sets were collected, giving the same cell constants and upon structure solution and refinement the same structure. The refinement of the best data set is reported here. Some atomic displacement parameters in compound **1** indicate prolate thermal ellipsoids which can be traced to motion perpendicular to the plane through the atoms, as indicated by the larger temperature factors in this (perpendicular) direction. In compound **1** only the O and C atom of the manganese-coordinated DMF solvent could be found and refined. The remaining $N(CH_3)_2$ part of the molecule is included in the recovered number of electrons in the void using the SQUEEZE routine in PLATON [18]. Compound **2** crystallized in the centrosymmetric space group $P2_1/n$ but was refined as a 2-component twin, based on the twofold rotation axis (0 0 1) [1 0 5] (in reciprocal space) [in direct space] using the twin law −1 0 0 0 −1 0 0 0 1 with HKLF 5 and a HKL-file generated from PLATON graphical menu though 'twinrotmat' yielding BASF 0.16. In the structures of **3**–**5** the value of sin(theta_max)/wavelength is less than 0.550. The porous MOF structures contain solvent-filled voids of comprising more than 50% of the unit cell volumes. Like in many other porous MOFs, also here the crystals did not diffract above theta 20°. Crystals of **5** did even diffract only to 2theta angles of 13°. In compound **3** and **4** RIGU restraints were applied with RIGU s1[0.004] s2[0.004] for all non-hydrogen atoms as enhanced rigid bond restraints with esds s1 for 1,2-distances and s2 for 1,3 [37]. Also, in **3** the single oxygen atoms O11, O12 and O13 on Cd1 are the donor atoms of coordinated DMF ligand molecules, which could not be refined due to disorder. Therefore the related electron density was removed with further residual electron density in the pores using the SQUEEZE routine in PLATON [18]. In compound **3**–**5** the flexible linker will assume slightly different conformations leading to disorder as indicated by different U_{eq} values of neighboring atoms, longer C—C bond lengths etc. Yet, the topology of the 3D metal-ligand network in **3**–**5** could be unequivocally determined.

Graphics were drawn with DIAMOND [38]. The crystallographic data have been deposited with the Cambridge Crystallographic Data Center (CCDC-numbers 1559378-1559382 for H_2L1 **2**, **4**, **1** and **3**, respectively). These data can be obtained free of charge *via* www.ccdc.cam.ac.uk/data_request/cif. For the structure of **5** refinement details are only reported here without structure deposition at CCDC due to low structure quality. See Supporting Information for further details of structure **5**.

4. Conclusions

A ditopic dicarboxylate linker with an urea group built-in gives rise to coordination polymeric and metal-organic framework structures. For the linker $L2^{2-}$ = 4,4′-(carbonylbis(azanediyl))bis(3-methylbenzoate) isostructural or isoreticular MOF structures are obtained for the different metal atoms Mn^{2+}, $Zn^{2+}$and Cd^{2+}, indicating the exerted structure control by the linker. The dimensions of the linker create large voids in diamondoid, **dia** networks. Despite the resulting fourfold interpenetration, which is rare in MOF-structures, about 50% of solvent accessible volume remains. In order to obtain permanently porous structures with urea-functionality in the linker the framework stability needs to be increased, however. At present, the inherent linker flexibility around the urea group gives rise to loss of crystallinity and void volume upon activation through solvent exchange and drying. We will now tackle this problem through judicious linker modification with rigidification.

Acknowledgement

The work was supported by the German Science Foundation (DFG – Germany) through grant Ja-466/29-1.

Appendix A. Supplementary data

Supplementary data associated with this article can be found, in the online version, at http://dx.doi.org/10.1016/j.ica.2017.09.029.

References

[1] (a) G. Maurin, C. Serre, A. Cooper, G. Férey, Chem. Soc. Rev. 46 (2017) 3104–3107;
(b) T. Kitao, Y. Zhang, S. Kitagawa, B. Wang, T. Uemura, Chem. Soc. Rev. 46 (2017) 3108–3133;
(c) K.K. Gangu, S. Maddila, S.B. Mukkamala, S.B. Jonnalagadda, Inorg. Chim. Acta 446 (2016) 61–74;
(d) S. Quaresma, V. Andre, A. Fernandes, M.T. Duarte, Inorg. Chim. Acta 455 (2017) 309–318.
[2] (a) K. Adil, Y. Belmabkhout, R.S. Pillai, A. Cadiau, P.M. Bhatt, A.H. Assen, G. Maurin, M. Eddaoudi, Chem. Soc. Rev. 46 (2017) 3402–3430;
(b) W.P. Lustig, S. Mukherjee, N.D. Rudd, A.V. Desai, J. Li, S.K. Ghosh, Chem. Soc. Rev. 46 (2017) 3242–3285;
(c) A. Herbst, C. Janiak, CrystEngComm 19 (2017) 4092–4117.
[3] (a) J. Dechnik, J. Gascon, C.J. Doonan, C. Janiak, C.J. Sumby, Angew. Chem. Int. Ed. 56 (2017) 9292–9310. Angew. Chem. 129 (2017) 9420–9439.;
(b) S. Singha, S.K. Maity, S. Biswas, R. Saha, S. Kumar, Inorg. Chim. Acta 453 (2016) 321–329;
(c) J. Dechnik, C.J. Sumby, C. Janiak, Cryst. Growth Des. 17 (2017) 4467–4488;
(d) L.F. Marques, H.P. Santos, C.C. Correa, J.A.L.C. Resende, R.R. da Silva, S.J.L. Ribeiro, F.C. Machado, Inorg. Chim. Acta 451 (2016) 41–51;
(e) N. Goel, Inorg. Chim. Acta 450 (2016) 330–336;
(f) S. Nießing, C. Czekelius, C. Janiak, Catalysis Commun. 95 (2017) 12–15.
[4] (a) F. Jeremias, D. Fröhlich, C. Janiak, S.K. Henninger, New J. Chem. 38 (2014) 1846–1852;
(b) C. Janiak, S.K. Henninger, Chimia 670 (2013) 419–424;
(c) C. Janiak, S.K. Henninger, Nachr. Chemie 61 (2013) 520–523;
(d) S.K. Henninger, F. Jeremias, H. Kummer, C. Janiak, Eur. J. Inorg. Chem. (2012) 2625–2634;
(e) D. Fröhlich, E. Pantatosaki, P.D. Kolokathis, K. Markey, H. Reinsch, M. Baumgartner, M.A. van der Veen, D.E. De Vos, N. Stock, G.K. Papadopoulos, S.K. Henninger, C. Janiak, J. Mater. Chem. A 4 (2016) 11859–11869;
(f) F. Jeremias, D. Fröhlich, C. Janiak, S.K. Henninger, RSC Adv. 4 (2014) 24073–24082.
[5] P.W. Siu, Z.J. Brown, O.K. Farha, J.T. Hupp, K.A. Scheidt, Chem. Commun. 49 (2013) 10920–10922.
[6] C. Volkringer, S.M. Cohen, Angew. Chem. Int. Ed. 49 (2010) 4644–4648.
[7] X.W. Dong, T. Liu, Y.Z. Hu, X.Y. Liu, C.M. Che, Chem. Commun. 49 (2013) 7681–7683.
[8] A.A. Tehrani, L. Esrafili, S. Abedi, A. Morsali, L. Carlucci, D.M. Proserpio, J. Wang, P.C. Junk, T. Liu, Inorg. Chem. 56 (2017) 1446–1454.
[9] X.-J. Wang, J. Li, Q.-Y. Li, P.-Z. Li, H. Lu, Q. Lao, R. Ni, Y. Shi, Y. Zhao, CrystEngComm 17 (2015) 4632–4636.
[10] Q.-Y. Li, Y. Quan, W. Wei, J. Li, H. Lu, R. Ni, X.-J. Wang, Polyhedron 99 (2015) 1–6.
[11] J.M. Roberts, B.M. Fini, A.A. Sarjeant, O.K. Farha, J.T. Hupp, K.A. Scheidt, J. Am. Chem. Soc. 134 (2012) 3334–3337.
[12] A.A. Tehrani, S. Abedi, A. Morsali, J. Wang, P.C. Junk, J. Mater. Chem. A 3 (2015) 20408–20415.
[13] R.S. Forgan, R.J. Marshall, M. Struckmann, A.B. Bleine, D.-L. Long, M.C. Berninib, D. Fairen-Jimenez, CrystEngComm 17 (2015) 299–306.
[14] C.A. Fernandez, P.K. Thallapally, R.K. Motkuri, S.K. Nune, J.C. Sumrak, J. Tian, J. Liu, Cryst. Growth Des. 10 (2010) 1037–1039.
[15] T.-F. Liu, J. Lu, R. Cao, CrystEngComm 12 (2010) 660–670.
[16] F.C. Pigge, CrystEngComm 13 (2011) 1733–1748.

[17] W.C. Drewe, R. Nanjunda, M. Gunaratnam, M. Beltran, G.N. Parkinson, A.P. Reszka, D.W. Wilson, S. Neidle, J. Med. Chem. 51 (2008) 7751–7767.
[18] A.L. Spek, Acta Crystallogr. Section D 65 (2009) 148–155; PLATON – A Multipurpose Crystallographic Tool, Utrecht University, Utrecht, The Netherlands, A. L. Spek (2008); Windows implementation: L.J. Farrugia, University of Glasgow, Scotland, Version 40608, (2008).
[19] M.C. Etter, Acc. Chem. Res. 23 (1990) 120-126; M.C. Etter, J.C. MacDonald, J. Bernstein, Acta Crystallogr. B 46 (1990) 256-262; M.C. Etter, J. Phys. Chem. 95 (1991) 4601-4610.
[20] E.I. Stiefel, G.F. Brown, Inorg. Chem. 11 (1972) 434–436.
[21] S. Banerjee, A. Ghosh, B. Wu, P.-G. Lassahn, C. Janiak, Polyhedron 24 (2005) 593–599.
[22] C. Heering, B. Francis, B. Nateghi, G. Makhloufi, S. Lüdeke, C. Janiak, CrystEngComm 18 (2016) 5209–5223.
[23] The three letter symbols, proposed by M. O'Keeffe, can be retrieved with examples and further information from the Reticular Chemistry Structure Resource database, http://rcsr.anu.edu.au/.
[24] (a) L. Carlucci, G. Ciani, D.M. Proserpio, T.G. Mitina, V.A. Blatov, Chem. Rev. 114 (2014) 7557–7580;
(b) V.A. Blatov, L. Carlucci, G. Ciani, D.M. Proserpio, CrystEngComm 6 (2004) 377–395;
(c) L. Carlucci, G. Ciani, D. Proserpio, Coord. Chem. Rev. 246 (2003) 247–289.
[25] (a) D.M. Proserpio, Nature Chem. 2 (2010) 435–436;
(b) L. Fang, M.A. Olson, D. Benítez, E. Tkatchouk, W.A. Goddard III, J.F. Stoddart, Chem. Soc. Rev. 39 (2010) 17–29;
(c) B. Xu, Z. Lin, L. Han, R. Cao, CrystEngComm 13 (2011) 440–443;
(d) K.A. Brown, D.P. Martin, R.L. LaDuca, CrystEngComm 10 (2008) 846–855;
(e) F. Luo, Y.-T. Yang, Y.-X. Che, J.-M. Zheng, CrystEngComm 10 (2008) 981–982;
(f) H.-P. Wu, C. Janiak, L. Uehlin, P. Klüfers, P. Mayer, Chem. Commun. (1998) 2637–2638.
[26] S.-T. Zhenga, G.-Y. Yang, Dalton Trans. 39 (2010) 700–703.
[27] M.-H. Zeng, Y.-X. Tan, Y.-P. He, Z. Yin, Q. Chen, M. Kurmoo, Inorg. Chem. 52 (2013) 2353–2360.
[28] G. Mehlana, G. Ramon, S.A. Bourne, Microporous Mesoporous Mater. 231 (2016) 21–30.
[29] A. Burgun, R.S. Crees, M.L. Cole, C.J. Doonana, C.J. Sumby, Chem. Commun. 50 (2014) 11760–11763.
[30] R.T. Lum, M. Cheng, C.P. Cristobal, I.D. Goldfine, J.L. Evans, J.G. Keck, R.W. Macsata, V.P. Manchem, Y. Matsumoto, S.J. Park, S.S. Rao, L. Robinson, S. Shi, W. R. Spevak, S.R. Schow, J. Med. Chem. 51 (2008) 6173–6187.
[31] H. Eckert, B. Forster, Angew. Chem. 99 (1987) 922–923.
[32] APEXII: Data collection program for the APEXII CCD area-detector system, Bruker Analytical X-ray Systems, Madison, Wisconsin, USA, 2010.
[33] SMART: Data Collection Program for the CCD Area-Detector System; SAINT: Data Reduction and Frame Integration Program for the CCD Area-Detector System. Bruker Analytical X-ray Systems, Madison, Wisconsin, USA, 1997.
[34] G.M. Sheldrick, SADABS, University of Gottingen, Gottingen, Germany, 1996.
[35] G.M. Sheldrick, Acta Crystallogr. A 64 (2008) 112–122.
[36] J. Newman, Acta Crystallogr. D 62 (2006) 27–31.
[37] A. Thorn, B. Dittrich, G.M. Sheldrick, Acta Crystallogr. A 68 (2012) 448–451.
[38] K. Brandenburg, DIAMOND (Version 4.4.0), Crystal and Molecular Structure Visualization, Crystal Impact – K. Brandenburg & H. Putz Gbr: Bonn, Germany, 2009–2017.
[39] H.D. Flack, M. Sadki, A.L. Thompson, D.J. Watkin, Acta Crystallogr. A 67 (2011) 21–34;
H.D. Flack, G. Bernardinelli, Chirality 20 (2008) 681–690;
H.D. Flack, G. Bernardinelli, Acta Crystallogr. A 55 (1999) 908–915;
H. Flack, Acta Crystallogr. A 39 (1983) 876–881;
S. Parsons, H.D. Flack, T. Wagner, Acta Crystallogr. B 69 (2013) 249–259.